THE JOURNAL OF PHYSICAL CHEMISTRY C

Article

Cite This: J. Phys. Chem. C 2017, 121, 27683−27692

pubs.acs.org/JPCC

Dielectric Behavior and Electro-Magnetic Coupling at Room Temperature in $BiFeO_3$/PVDF and $CoFe_2O_4$/PVDF Composites

Leila María Saleh Medina[†,‡] and R. Martín Negri*[,†,‡]

[†]Instituto de Química Física de Materiales, Ambiente y Energía (INQUIMAE), CONICET, Buenos Aires, Argentina

[‡]Departamento de Química Inorgánica, Analítica y Química Física, Facultad de Ciencias Exactas y Naturales, Universidad de Buenos Aires, Ciudad Universitaria, Pabellón II, INQUIMAE, C1428EGA Buenos Aires, Argentina

Supporting Information

ABSTRACT: The dielectric properties of composites formed by dispersions of two types of ceramic particles, $BiFeO_3$ (multiferroic) and $CoFe_2O_4$ (magnetic), in poly(vinylidene fluoride), PVDF, (which can present a ferroelectric phase) were studied at room temperature as a function of particle concentration. The characterization studies include determination of dielectric polarization curves in the presence of external magnetic fields, **H** (that is, **P**−**E** plots in the presence of **H**, where **P** is the dielectric polarization and **E** the external applied electric field). Impedance spectroscopy analysis shows the presence of several distributions of dipolar relaxation processes, some of which are assigned to charge rearrangements at the different interfaces of the system, for example at the ceramic-polymer interfaces. Negative magneto-electric coupling was observed at low ceramic proportion (where leakage currents are lower than 20 nA/cm^2), that is, decrease of **P** when applying **H**, $\left(\frac{\partial \mathbf{P}}{\partial \mathbf{H}}\right)_E < 0$. The negative coupling is opposite to previously observed for $BiFeO_3$ dispersed in a nonferroelectric matrix (styrene−butadiene-rubber, SBR) where $\left(\frac{\partial \mathbf{P}}{\partial \mathbf{H}}\right)_E > 0$. These results suggest a strong polymer−particle interaction, where the interfaces between the two components play a central role. The observation of negative magneto-electric suggests a matrix-mediated coupling, possibly through a magneto-striction mechanism at the ceramic-polymer interfaces. The description of magneto-electric coupling on the bases of magnetostriction effects leads to the conclusion that the results in PVDF and SBR are in agreement with positive magnetostriction, that is positive strains (elongation) when a magnetic field is applied.

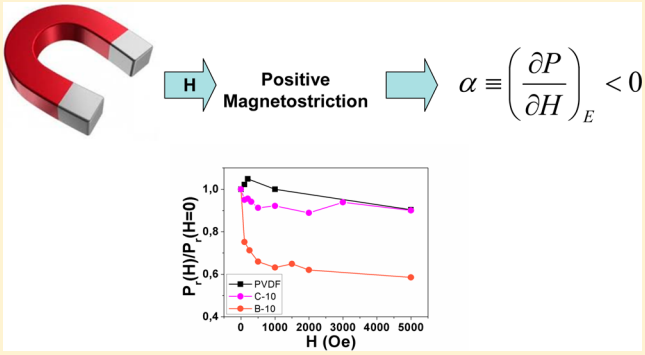

1. INTRODUCTION

Composites formed by dispersions of inorganic particles with different properties (conductive, dielectric and/or magnetic) in elastic polymer matrices are of high interest for their applications in flexible electronics.[1] Examples of application are mechanical stress sensors,[2] magnetic field sensors[3] and capacitors.[4] In such systems the major volume fraction is given by the organic component hence preserving the elastic properties, while the electric or magnetic properties are provided by the filler particles. It is desired to have control, even partial, of these properties by varying the proportion of incorporated particles. In some applications the matrix is inert and it simply provides an elastic medium in which to disperse the particles. That is the case of styrene−butadiene rubber (SBR) and polydimethylsiloxane (PDMS), previously used in our group to implement different devices based on particle/polymer composites.[2,5−7] In these works, magnetite−silver agglomerates (simultaneously magnetic and conductors) were dispersed in PDMS and SBR to implement both magnetic field sensors (based on magnetoresistivity) and mechanical stress sensors (based on piezoresistivity). $BiFeO_3$, a well-known multiferroic material which presents magnetic and electric orders at room temperature, was also incorporated into SBR to obtain elastic dielectrics for capacitors.[8] The features of impedance spectra were well accounted by modeling the composite by an R//C equivalent circuit, where the static dielectric constant, ε_s, increases with $BiFeO_3$ proportion. Dielectric-magnetic coupling was observed in these systems, that is, the possibility of modifying the dielectric polarization per unit volume, **P**, by applying an external magnetic field, **H**.

In other cases, it seems interesting to use matrices that are not inert but may present some ferrous order in the absence of particles. The paradigmatic organic material is poly(vinylidene fluoride), PVDF, a fluorocarbon-based polymer with multiple carbon−fluorine bonds. PVDF is very well-known for presenting a ferroelectric phase at room temperature, referred

Received: August 5, 2017
Revised: October 14, 2017
Published: November 10, 2017

DOI: 10.1021/acs.jpcc.7b07800
J. Phys. Chem. C 2017, 121, 27683−27692

as the β-phase, while maintaining its elastomer characteristics.[9] The proportion of β-phase can be enhanced by adding salts,[10,11] like $Mg(NO_3)_2{\cdot}6H_2O$, probably through hydrogen bonding that includes F atoms. It has been reported also that dispersing carbon nanotubes[12] and clays[13] in PVDF increases the proportion of ferrolelectric phase.

Different metal and ceramic materials have been incorporated to PVDF matrixes in order to improve the dielectric properties of PVDF.[14−16] Reddy et al. reported on preparation of a 50% w/w $BiFeO_3$−PVDF films by hot-press technique.[17] Moharana et al. reported on dielectric properties of a 10% w/w $BiFeO_3$−PVDF obtained by solution casting method.[18] Martins et al.[19] have analyzed the influence of $CoFe_2O_4$ and $NiFe_2O_4$ in the formation of β phase. In subsequent works of Martins et al.,[20,21] the magneto-electric effect was measured in similar composites up to 20% w/w of particles. The increase of β-phase when adding $CoFe_2O_4$ has been assigned by Martins et al.[19−21] to the interaction between the negatively charged surface of the particles and the positively CH_2 groups of PVDF, which may promote nucleation of ferroelectric domains.

The mentioned works indicate that strong interactions between particles and PDVF may be present in the composites. It is therefore of high interest for possible applications in flexible devices, to explore the possibility of synergism between properties of both components (polymer and filler), or matrix-mediated coupling of properties. Hence, in the present work we study the properties of PVDF composites formed by adding two different ceramic particles, $BiFeO_3$ and $CoFe_2O_4$. In the text, the term *ceramic* refers here to $BiFeO_3$ and/or $CoFe_2O_4$ particles. $BiFeO_3$ was selected for its multiferroic behavior at room temperature, displaying ferroelectricity and ferromagnetism; thus, an electro-magneto coupling is expected in $BiFeO_3$/PVDF composites. On the other hand, the $CoFe_2O_4$ nanoparticles present ferromagnetism, but not ferroelectricity, at room temperature, and results on $CoFe_2O_4$/PVDF composites are presented for comparison.

In previous works synthesis of $BiFeO_3$ and $CoFe_2O_4$ ceramics were reported, obtaining in both cases materials with high crystallinity and purity, whose magnetic and dielectric properties were well characterized.[22,23]

In spite of the potentiality of these composites as materials for inducing changes of the dielectric properties by the action of applied magnetic fields, there are no reports of dielectric polarization curves in the presence of magnetic fields, as far as we know. Some authors report magneto electric effect as voltage induction due to the application of an AC magnetic field. In this work and in our previous one,[8] the magneto electric effect is determined from the change in dielectric polarization curves ($\mathbf{P}-\mathbf{E}$) under different static magnetic fields ($\mathbf{H}$). Therefore, the aims of the present work are to characterize the dielectric response and to explore the electro-magnetic coupling of ceramic/PVDF composite films at room temperature.

2. MATERIALS AND METHODS

2.1. Preparation of Films. The synthesis and characterization of $BiFeO_3$ and $CoFe_2O_4$ ceramics has been reported in previous articles of the group.[22,23] The average particle size distributions of the synthesized ceramics used here are 40 and 30 nm for $BiFeO_3$ and $CoFe_2O_4$ particles, respectively. However, when the particles are dispersed into the polymer matrix, agglomerated of particles are formed with average sizes about 200 nm (for W = 10) to 500 nm (for W = 275) with dispersions about 50 and 100 nm, respectively. The areal density of the aggregated in the matrix when observed in images recorded by AFM or SEM from the top of the films is in the order of 10^{-2} μm^{-2}.

Poly(vinylidene fluoride) (PVDF; $(CH_2CF_2)_n$; CAS Number: 24937-79-9; average $M_w \sim 534\,000$ by GPC; $n \sim 8000$), powder was purchased from Sigma-Aldrich.

The nomenclature used in the present work for the different composite films is the following. Composites of $BiFeO_3$ in PVDF are indicated as "B" films, while those of $CoFe_2O_4$ in PVDF as "C" films. The mass proportion of particles in the composite is given by W, where W ≡ 100 (mass of ceramic)/(mass of PVDF). Along the text, composites are referred as "B−W" or "C−W" films. For instance, "B-100" indicates a composite film of $BiFeO_3$/PVDF with W = 100 (prepared in DMF and adding $Mg(NO_3)_2{\cdot}6H_2$, as described below).

When calculated as filler mass fractions, the considered range for both fillers goes from 9 to 73% *w/w*. Below 9% *w/w* no filler effects were noticed, while above 75% w/w the composites presented large macroscopic inhomogeneities or sometimes cracking. Beyond these technical aspects, the important parameter for describing filler effects is the filler's *volume* fraction, φ_{filler}, which is estimated from the filler mass fraction, $\varphi_{mass\ filler}$ by $\varphi_{filler} = \varphi_{filler}^{mass}\frac{\delta_{composite}}{\delta_{filler}}$, where $\delta_{composite}$ and δ_{filler} are the densities of composite and filler, respectively. The density of the composites was evaluated from weighting and volume determination at several filler proportions, rendering values about 1.1−1.3 gcm^{-3}. The density of filler is estimated similar to the bulk density of the respective ceramic; 8 $gcm^{-3}$for $BiFeO_3$ and 5 gcm^{-3} for $CoFe_2O_4$. These calculations give the range for φ_{filler}: 1 to 12% V/V for $BiFeO_3$ and from 2 to 19% V/V for $CoFe_2O_4$ To expand these ranges toward larger volume fractions requires to prepare composites with filler mass proportion about 75% w/w, finding the practical difficulties mentioned above related to sample preparation. On the other hand, to expanded it toward lower filler proportions requires to study composites with mass proportion lower than 9%, where the sensitivity to filler effects on the dielectric properties is low in case of using polymer matrixes with large dielectric constant (or even ferroelectric) as in the case reported here of β-phase PVDF.

To prepare the films, 100 mg of PVDF (Sigma-Aldrich) were dissolved in dimethylformamide (DMF) under sonication to obtain a clear solution 5% w/w PVDF:DMF. Then, $Mg(NO_3)_2{\cdot}6H_2O$ was added until complete dissolution (20% w/w salt:PVDF), since it has been shown that this concentration maximizes the proportion of β phase.[11] Once PVDF and $Mg(NO_3)_2{\cdot}6H_2O$ were dissolved, the ceramic particles were added to form a suspension. These suspensions were kept under permanent stirring while DMF was left to partially evaporate until obtaining a viscous fluid which was deposited by spin coating onto aluminum substrates (Al, Sigma-Aldrich). Typical speeds for spin coating were 300−500 rpm during 10 s. Afterward, the films were dried at 125 °C for 15 min. All solvents and reagents were of analytical quality. The average thicknesses of the films ($\langle L \rangle$) were in the range of 30−300 μm, dependent on speed of the spin coating process, ceramic concentration, etc. The area of the samples was 1 cm^2. These areas are larger than the top electrode area, A (0.2 cm^2), used during all dielectric determinations.

DOI: 10.1021/acs.jpcc.7b07800
J. Phys. Chem. C 2017, 121, 27683−27692

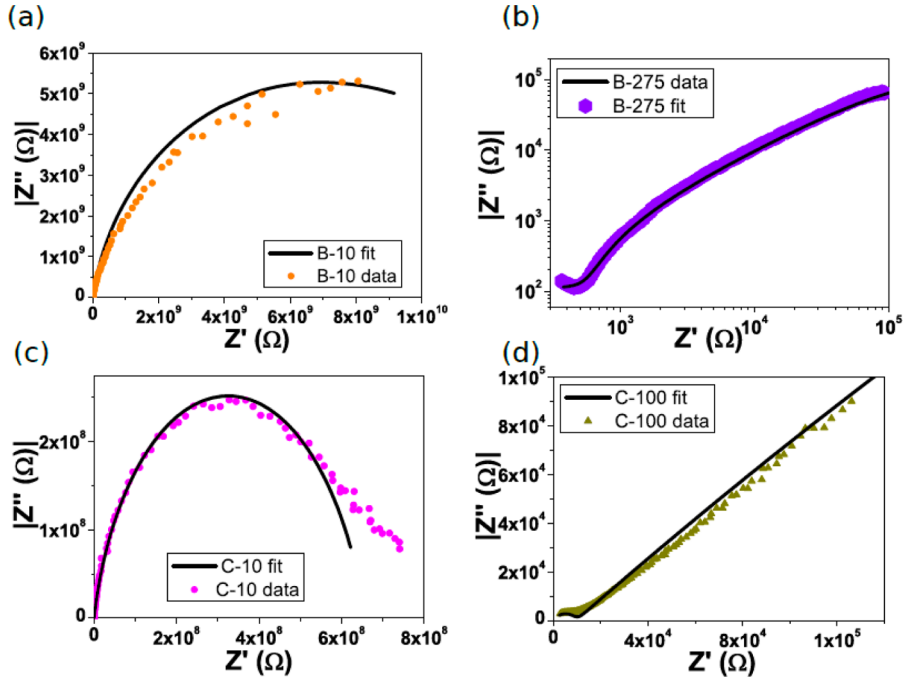

Figure 1. Real (Z') vs imaginary (Z'') impedance components, for (a) B-10, (b) B-275, (c) C-10, and (d) C-100. Full lines represent the fitting by circuit displayed in Figure 2.

2.2. Instrumentation. Spin coating was performed with a SPIN-1200D (MIDAS SYSTEM) spin coater at room temperature.

The thicknesses of the dried films were measured using a surface profilometer (Veeco, model Dektak 150) whose instrumental details are described in a previous work.[8] The thickness of the film, L, was measured as a function of the scanned distance and the average values of L, referred as $\langle L \rangle$, were calculated within a defined scanning distance range (500−1500 μm, depending on the sample) starting from at least 100 μm from the edge of the film.

Fourier transformed infrared (FTIR) spectra (4000−400 cm^{-1}; resolution 4 cm^{-1}) were acquired with a Nicolet 8700 equipment using a Smart Orbit ATR accessory (single horizontal reflection with diamond crystal) and a DTGS detector.

The structure of the dried composite films was investigated by scanning electron microscopy (SEM) using a field emission scanning electron microscope (FESEM; Zeiss Supra 40 Gemini).

The AC-dielectric behavior as a function of frequency, f, was studied by impedance analysis spectroscopy (ISA) for f between 0.1 Hz and 1 MHz. The ISA experiments were carried on a TEQ-4 potentiostat (Argentina), applying sinusoidal waves of frequencies f, keeping fixed the peak-to-peak voltage at 0.5 V. The primary data obtained from impedance spectroscopy are the real and imaginary components (Z' and Z'', respectively) of the complex impedance $Z(\omega) = Z'(\omega) + jZ''(\omega)$, as functions of f or ω ($\omega \equiv 2\pi f$; j is the imaginary number). From that, the modulus of Z, $|Z| = \sqrt{Z'^2 + Z''^2}$ and the phase angle ϕ (with $tg(\phi) \equiv \frac{|Z''|}{|Z'|}$) are obtained.[24]

The DC-dielectric characterization as a function of the applied electric field **E** was performed using a Precision LC Material Analyzer (Radiant Technologies). Polarization curves (**P**−**E** curves) were taken at a sampling rate of 1562.5 Hz by applying a bipolar triangular wave (0; + V_{max}; −V_{max}; 0). Density current plots of DC-currents (**J**−**E** plots) were recorded with the LC analyzer. In these cases the bottom electrode (Al) was connected to ground.

The effect of an external magnetic field on the dielectric properties (electro-magnetic coupling) was determined by inserting the sample between the pole pieces (10 cm diameter) of a Varian low impedance electromagnet (model V3703). These kinds of electromagnets are known to provide highly homogeneous steady magnetic fields, **H** (expressed in Oe), that were measured with a Group3 DTM-133 Digital Teslameter. A specially designed set up was implemented in order to place the samples between the electromagnet and to provide the electrical contacts for establishing communication with the Precision LC Material Analyzer. In this way it was possible to register **P**−**E** curves simultaneously with the application of a given magnetic field **H**, whose value can be arbitrarily fixed.

The behavior of the composites as ac-circuit components in the range 100 kHz-7 MHz was studied by analyzing the response of the samples in series with a 1 kΩ commercial resistance to a sinusoidal wave generated with a Siglent SDG 1050 generator. In these experiments the response of the circuit was determined with a Hantek MS05062D dual-channel oscilloscope (60 MHz broadband). The oscilloscope probes used at the test points were previously calibrated against a square waveform internal reference signal by adjusting the probe's capacitance until obtaining input signals that match almost exactly the reference waveform, thus minimizing probing effects.

3. RESULTS AND DISCUSSIONS

3.1. Ferroelectric Phase Formation. PVDF presents two main phases, referred as α and β phases. The β-phase (F atoms in all-trans conformation) is required to have a ferroelectric behavior. The relative proportion of both phases can be

DOI: 10.1021/acs.jpcc.7b07800
J. Phys. Chem. C 2017, 121, 27683−27692

determined from the FTIR spectra,[9] since both phases have characteristic peaks at 763 and 840 cm^{-1} for α and β, respectively. A relationship has been proposed[12,25] to quantify the proportion of β phase: $F(\beta) = \frac{A_{840}}{A_{840} + 1.23A_{763}}$, where A_{840} is the absorbance at 840 cm^{-1} and A_{763} is the absorbance at 763 cm^{-1}.

The FTIR spectra indicate that in pristine PVDF (without adding any other compound) only about 53% of the material is in the β phase, calculated from $F(\beta)$. The dissolution of the polymer in DMF and the addition of $Mg(NO_3)_2{\cdot}6H_2O$ considerably increase the intensity and number of peaks corresponding to the β phase (Figure S1a, Supporting Information). In fact, we observed that the proportion of β phase (calculated from $F(\beta)$) in all cases is larger than 90% in the samples prepared in DMF with $Mg(NO_3)_2{\cdot}6H_2O$, demonstrating that the preparation method described in the previous section renders a large increase of the β phase. Addition of ceramics further increases the amount of β phase with percentages about 100% of β-phase for B-100 films (see Figure S1b). Although the involved mechanisms are not well understood yet, the presence of adsorbed water molecules and filler particles seems to be responsible for β-phase formation trough polar and hydrogen bond interactions with F atoms in the polymer chains. For instance, it has been suggested that $Mg(NO_3)_2{\cdot}6H_2O$ acts as β phase nucleation sites due to the formation of hydrogen bonds.[13] Concerning the effect of adding particles, our results are consistent with reports of β phase increase after incorporating inorganic fillers such as carbon nanotubes or clays.[12,13,25] The results presented here indicate that β-phase formation is favored by the addition of $BiFeO_3$ or $CoFe_2O_4$ to PVDF. This is in agreement with previous report for the case of $CoFe_2O_4$/PVDF composites[26] and is extended here to the case of $BiFeO_3$/PVDF.

Summarizing, the composites studies in the present work are mainly in the β-phase (the percentage of other phases is less than 1%).

3.2. Impedance Spectroscopy. Figure 1 shows imaginary (Z'') vs real (Z') components of impedance and the corresponding fits by the circuit showed in Figure 2 for PVDF−Mg, B−W, and C−W films.

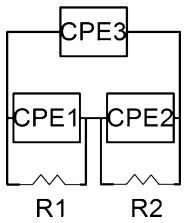

Figure 2. Equivalent circuit used to fit impedance spectroscopy data as a function of frequency, at low electric fields ($E_{peak\text{-}to\text{-}peak}$ < 0.1 kV/cm). CPE: constant phase element.

The impedance behavior is analogous for samples B and C, Z' and Z'' decreases with frequency, although the sensitivity to ceramic concentration (given by W) is larger for B-samples than C-samples, which is probably related to that B samples contains a multiferroic filler ($BiFeO_3$). Figures S2 and S3 shows data and fits of $|Z|$ and ϕ as a function of f, for B and C samples, respectively.

Irrespective of the ceramic and W, distorted semicircles are obtained, which suggests the presence of dipoles and charge distributions as discussed in the following paragraphs. In fact, it is not possible to adjust the observed impedance responses by using simple circuit elements such as resistances (R) and capacitances (C) only. If the frequency response were well accounted by an $R//C$ circuit, then only one kind of dipole relaxation process should occur in the material and with only one characteristic relaxation time = RC. That is, in the $R//C$ systems there is only one kind of relaxation process having a delta distribution with relaxation time equal to RC. Since this is not in agreement with the experimental evidence of the ceramic/PVDF composite, then the so-called *constant phase elements* (CPE) were incorporated as circuit elements in order to fit the impedance spectra. The CPE elements use to account for systems where a distribution of dipoles and charges are present. The impedance of those elements, Z_{CPE}, is given by $Z_{CPE} = \frac{1}{P(j\omega)^n}$, using MKSI units. These elements are associated with the presence of a distribution of relaxation times. The parameters P and n are empirical positive coefficients. The coefficient n varies between 0 (pure resistance) and 1 (pure capacitance). Several parallel and series combinations of R and Z_{CPE} elements were tried in order to fit the experimental data. The equivalent circuit that best fits the impedance spectroscopy data for both ceramics (B and C), all proportions (W from 0 to 275), in the whole frequency range (from 0.1 Hz to 1 MHz), and at low electric fields ($E_{peak\text{-}to\text{-}peak}$ < 0.1 kV/cm),is shown in Figure 2. As noted, more than one CPE element was required for fitting the data, suggesting that more than one relaxation distribution is present in the considered frequency range.

The recovered values of the circuit elements, obtained from fitting the experimental data, are shown in Table 1. Figures 1, S2 and S3 show the excellent fits of experimental impedance spectroscopy data recovered using the equivalent circuit of Figure 2.

Table 1. Parameters Recovered from Fitting Impedance Data, with Primary Data (Z' and Z'') Expressed in Ohms[a]

sample	low-W PVDF−Mg, B-10, B-100 and C-10	high-W B-275, C-100, and C-275
$R_1 + R_2$ (Ω)	10^9−10^{10}	10^5−10^6
n_3	0.8−0.9	0.4−0.6
n_1	0.5−0.9	0.5−0.6
n_2	0.5−0.9	0.2−0.8
P_3	10^{-12}−10^{-10}	10^{-10}−10^{-5}
P_1	10^{-11}−10^{-7}	10^{-6}−10^{-7}
P_2	10^{-11}−10^{-10}	10^{-10}−10^{-8}

[a]The indicated ranges correspond to variability from five replicates of each concentration.

It can be observed an important concentration effect for samples with the largest W, for instance W > 100 for B-films and $W \geq 100$ for C-films. On the other hand, at lower values of W the relatively erratic variation with W of impedance data can be assigned to inhomogeneities due to sample preparation, thus these variations between samples are not considered statistically representative. Therefore, samples are classified into two groups, referred in Table 1 as low-W and high-W (for both, B and C-films) on the basis of their impedance response. The different impedance behavior of these groups is clearly observed by simple visual inspection in Figures 1, S2, and S3: the plots at the left side are typical for samples of the low-W group, while

DOI: 10.1021/acs.jpcc.7b07800
J. Phys. Chem. C 2017, 121, 27683−27692

those at the right side correspond to the high-W. Note also that all features of low-W plots (left side) keep partially some qualitative characteristics corresponding to an $R//C$ circuit: (i) the Cole plots (Z' vs Z'') displays a semicircle shape; (ii) ϕ increases with f up to reach a plateau close to 1.5 radians ($\pi/2$); (iii) the Bode plots (log|Z| vs log f) goes from a plateau at low f and then decreases linearly at high frequencies. This is associated with the fact that $n_3 \approx 0.8-0.9$ is closer to 1 (which correspond to $R//C$ circuit) for low-W samples, while clearly far from 1 in high-W samples ($n_3 \approx 0.4-0.6$). Nevertheless it is important to remark that in fact $n_3 < 1$ was always recovered (the slope of the Bode plots is systematically lower than 1, the predicted value for an $R//C$ circuit, in all samples of the low-W group), that is, and $R//C$ does not provide an appropriate quantitative nor qualitative description in the whole range of frequencies.

The deviations from an $R//C$ behavior are even larger in the high-W group (right sides of Figures 1,S2, and S3). The difference in behavior between low and high W groups can be analyzed also by looking at the recovered P_i and n_i values. For low-W samples, resistivities are quiet large (10−100 GΩ·cm), $P_i \leq 10^{-9}$ and $n_i \geq 0.5$. This is in agreement with the statement that for low-W groups, although pure capacities elements can never be used for fitting data, the response still remains some similarities to an $R//C$ (with high R and low C). On the other hand, in the high-W group, resistivities are lower than 10^{-1} GΩ·cm, $P_i \geq 10^{-9}$ (and P_1 and P_2 differs in orders of magnitude) and $n_i \leq 0.6$. This indicates important distortions from R//C behavior and relative large dielectric losses for the high-W group. Consider for instance the B-samples, noting that (a) R(B-275) ≪ R(low-W) suggesting larger DC-leakage currents for B-275; (b) P_3(B-275) ≫ P_3(low-W), indicating larger ac-currents for B-275.

Actually, the characteristics observed in the low-W groups are already present in films without ceramics (samples PVDF−Mg). That is, in the PVDF−Mg matrix where the β-phase predominates, there are distributions of relaxation times which can be assigned to the mentioned processes: rearrangements of interfacial charge between domains (including interfaces $\beta-\beta$, $\beta-\alpha$, and $\alpha-\alpha$) and relaxations of dipole moments of polymer chains. When ceramics are incorporated, new interfaces between the ceramics and the polymer are formed, which generates new distributions of relaxation processes superimposed to the existing ones in PVDF matrix, making difficult to perform a quantitative analysis of the perturbations introduced by adding ceramics at low proportions. Nevertheless, our results point out some changes due to the presence of ceramics at low proportions. For example, we have consistently observed that maxima of the Z'' function are shifted toward lower frequencies for samples B and C with respect to PVDF. The incorporation of ceramics at low concentrations induces the slowing down of the relaxation processes due to the heterogeneity present in the samples, when observed by impedance spectroscopy.[27] This is due, probably, to processes at the ceramic/polymer interfaces.

Recently Dash et al.[28] reported the dielectric behavior of $BiFeO_3$/PVDF composites as a function of filler concentration (data on $CoFe_2O_4$/PVDF were not presented). The systems studied by these authors have a more complex morphology than those described here since their composites are not present in one major phase (the β-phase) but in three polymorphic phases (α, β, γ) whose relative proportions changes with filler concentration. A continue change of the dielectric function $\varepsilon'(\omega)$ with $BiFeO_3$ concentration was reported, while we observe (Figure S4) here that the change of dielectric functions with filler concentration is abrupt above a given concentration threshold (which depends on the filler), associated with classification of samples in low-W and high-W groups. Although no mathematical model for impedance spectroscopy data was presented in the cited work, which could be compared to the one presented here, it is not possible to discard that the differences are due to the presence of different phases in the considered composites.

For applications of these materials in electronics it is also worth to analyze the loss dissipation factor, which is generally given by $\mathrm{tg}(\phi) \equiv \frac{|Z''|}{|Z'|}$, with the requirement $\mathrm{tg}(\phi) < 1$ in the largest possible frequency range, for appropriated real devices. This condition is satisfied in the low-W group for frequencies above 1 Hz (B-samples) and 10 Hz (C-samples) (values of ϕ are shown in Figures S2 and S3). On the other hand, films in the high-W group do not satisfy $\mathrm{tg}(\phi) < 1$ for any frequency. This indicates that (for samples in the high-W group) the energy introduced when applying an ac-cycle will not be stored as polarized charges but mainly dissipated as heat (Joule dissipation).

Summarizing, impedance spectroscopy shows the complicated dielectric behavior of PVDF composites in comparison to those formed in SBR or PDMS matrixes. The experimental results are compatible with the presence of more than one distribution of dipole moments and charges, which are already present in PVDF in absence of fillers. The relaxation processes at the lowest frequencies are associated with charge distributions at interfaces while those at the largest frequencies to dipole moments of the polymer matrix. Average relaxation times become slightly slower when adding ceramics at low proportions and a change from more "dielectric-like" to more "conductive-like" regime appears at volume fractions larger than 0.1.

3.3. Incorporation of Films As Electronic Components into a Simple AC Circuit. Films were included as impedance in series with a loading resistance, R_L (1 kΩ). An AC field V_{in} (4 V peak-to peak) was applied and the AC voltage on the film, V_{out}, was determined as a function of ω up to 6.5×10^7 rad s^{-1}. The ratio (V_{out}/V_{in}) as a function of ω is shown in Figure 3 for samples B and C.

A large decrease of (V_{out}/V_{in}) for frequencies in the megahertz range is observed as expected from the large decrease of Z' and Z'' with f in that range. At the lower frequencies Z' and Z'' are several orders of magnitude larger than R_L and (V_{out}/V_{in}) ≈ 1.

When frequency increases, Z' and Z'' decrease, and in the megahertz range they are of the same order of magnitude than R_L (or even slightly less for B-275 films) and (V_{out}/V_{in}) < 1. Note also in Figure 3 that the influence of W on (V_{out}/V_{in}) is larger for B-samples than C-films, as expected since Z' and Z'' are more sensitive to W in B-samples.

3.4. DC Behavior: Leakage Currents. In previous sections, the dielectric behavior as a function of the frequency was studied, using AC-stimulus of low electric field, $E_{peak\text{-}to\text{-}peak} \leq 0.1$ kVcm^{-1}. In this and next sections the dielectric response at cero-frequency (DC) in an extended range of electric fields, **E**, are studied (**E** up to 10 kVcm^{-1}). Figure 4 shows DC leakage current plots. It can be seen that at **E** = 2 kVcm^{-1}, the DC-current density, **J**, is about 1.0×10^{-2} and 5.0×10^2 μA cm^{-2} for samples B-10 and B-275, respectively, that is there is an

DOI: 10.1021/acs.jpcc.7b07800
J. Phys. Chem. C 2017, 121, 27683−27692

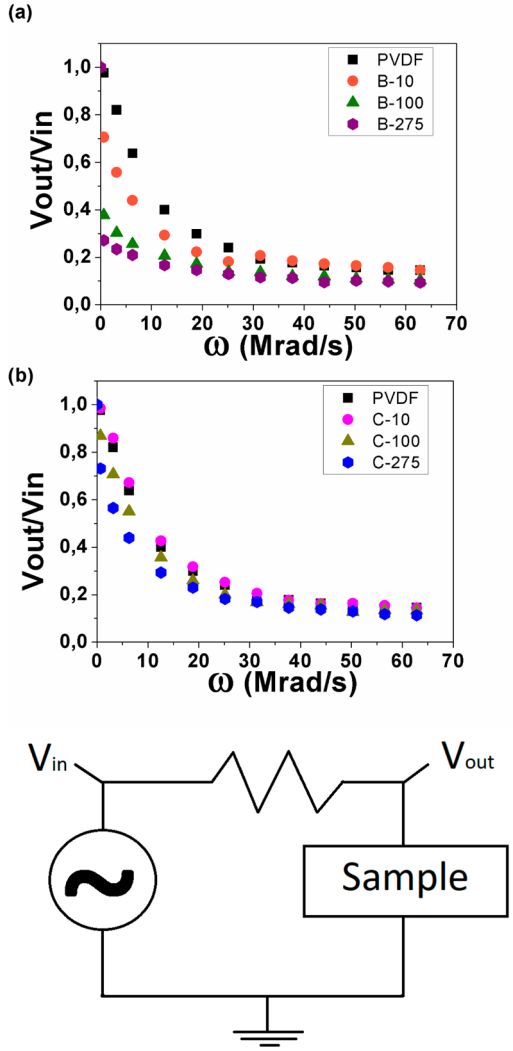

Figure 3. AC-response, (V_{out}/V_{in}), of films in series with a resistance R_L (1 kΩ). (a) $BiFeO_3$/PVDF; (b) $CoFe_2O_4$/PVDF.

increase in **J** of 4 orders of magnitude when comparing samples in the low-W and high-W groups. The DC-conductivities, σ_{DC}, are lower than 10^{-10} and 10^{-4} Ω^{-1} cm^{-1} for B-10 and B-275, respectively. Similar results hold for C-samples. Thus, leakage currents are several orders of magnitude larger in the high-*W* group than in the low-*W* group, which is in agreement with the picture that large proportion of ceramics favors the formation of conduction paths.

3.5. Ferroelectric Behavior and Electro-Magnetic Coupling. Dielectric polarization curves in the absence of external magnetic fields are shown in Figure 5 for different ceramic/PVDF composites. Dielectric hysteresis in the **P-E** plots of PVDF−$Mg(NO_3)_2{\cdot}6H_2O$ samples, in the absence of particles, is difficult to observe. This may be due to a lack of instrumental sensitivity at the relatively low electric fields used here. For instance, coercive fields of PVDF films have been reported in ranges larger than 300 kV/cm,[29−31] while the maximum field applied in the present work is only 100 kV/cm when applying 100 V (the maximum voltage allowed in the LC device) in the thinnest prepared films. In other words, although the main phase in PVDF−$Mg(NO_3)_2{\cdot}6H_2O$ is the *β*-phase, which is a needed requirement for getting a ferroelectric behavior, it seems that the low sensitivity of the instrumental conditions do not allow to observe a ferroelectric loop in the **P**−**E** plots of that samples.

When particles are added at low proportions (low-W groups), ferroelectric cycles appears, but a relatively low hysteresis is observed, perhaps because of the mentioned lack of sensitivity for using electric fields far from saturation (Figure 5). In the case of high-W group, the **P**−**E** plots may be highly influenced by the leakage currents, therefore the respective plots should be taken with care. Thus, the following discussion is restricted to the low-W group, where leakage currents (in DC and AC) are minimized.

In a few samples we reached electric fields closed to 100 kV/cm, which are actually very thin samples. Note that for reported data in Figures 4 and 5, the largest electric field obtained was only 6 kV/cm, actually. These values are similar to that used in the recent article by Mishra et al.[32] To reach larger fields it is necessary to use kilovolt sources or to reduce the thickness up to orders of 100 nm. However, it must be noted that, in the present system, it is not straightforward to obtain **P**−**E** curves where coercitivity and saturation can be observed. For example, the coercive electric field of PVDF has been reported about 300 kV/cm. Thus, fields close to 1000 kV/cm are needed to observe the complete hysteresis loop up to reach saturation of ferroelectric response. Therefore, to obtain those large fields while keeping the same thickness, voltage sources about 15 kV must be used, which are not available in commercial LC devices. Even if those voltages were applied, then leakage currents become very large, introducing distortions and artifacts in the **P**−**E** curves. Another factor to consider when using very larger fields is electrical breakdown.

The **P**−**E** responses of $BiFeO_3$/PVDF composites at the low-*W* group decreases in the presence of an external magnetic field, **H**, a negative magneto-electric (**ME**) coupling. This effect was observed systematically in all samples and is presented here as plots of relative change in the remanence polarization (P_R) as a function of **H**, only for the low-*W* group (Figure 6).

The assignation of this effect to the possible influence of **H** on the leakage currents is discarded for several reasons: leakage currents are low in the low-W group, no dependence with magnetic field of leakage currents was observed, the matrix (PVDF−Mg) and filler ($BiFeO_3$) do not present magneto-resistivity, and Hall-effects are not expected since **H** and **E** are parallels. Samples PVDF−Mg and C-10 present small and erratic behaviors (and remanence has large errors in PVDF−Mg). **ME** effects are clearly observed in C-10 and C-100 samples with similar values of $P_R(\mathbf{H})/P_R(H = 0)$ (not shown for C-100, for clarity).

The origin of **ME** effects in PVDF-filler particles is a matter of debate. Anithakumari et al.,[33] following Nan[34] suggest that **ME** in ferroelectric phases of PVDF loaded with magnetic fillers may be assigned to magnetostriction effects resulting from a complex process associated with the alignment of magnetic domains of magnetic fillers upon application of an external magnetic field. The application of **H** may produce therefore a stress of the neighboring ferroelectric PVDF phase, with consequent rearrangement of interfacial charges and hence inducing changes of **P**. These magnetostriction effects can be given, for instance, by modification of the distances between ions of the ceramics (currently a decrease) or between ceramic ions and F atoms of PVDF, under the presence of **H**. This hypothesis must be tested in future works, although was recently mentioned by Anithakumari et al.[33] and is also supported by few studies concerning magnetostriction effects.

DOI: 10.1021/acs.jpcc.7b07800
J. Phys. Chem. C 2017, 121, 27683−27692

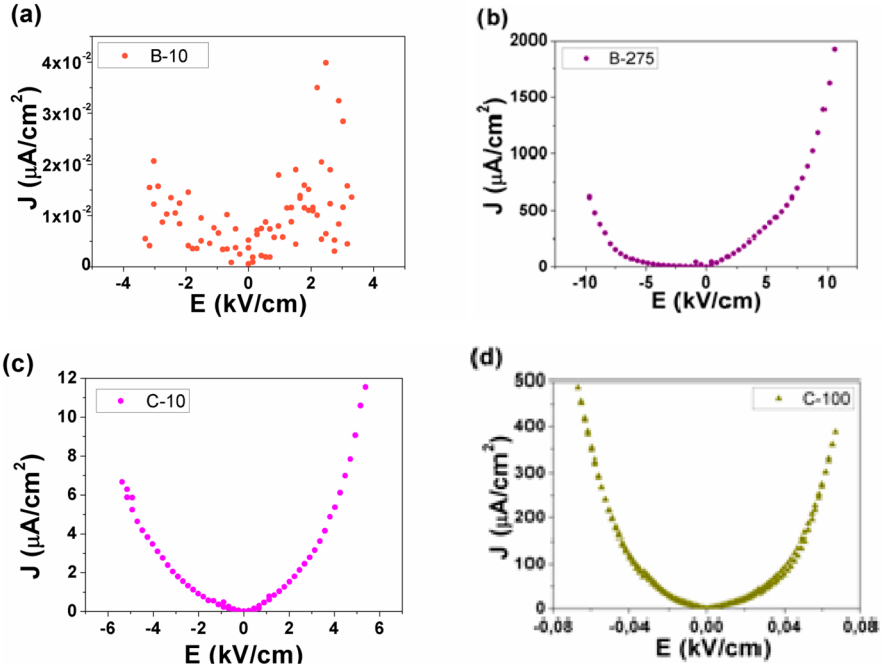

Figure 4. DC leakage currents for different B and C samples.

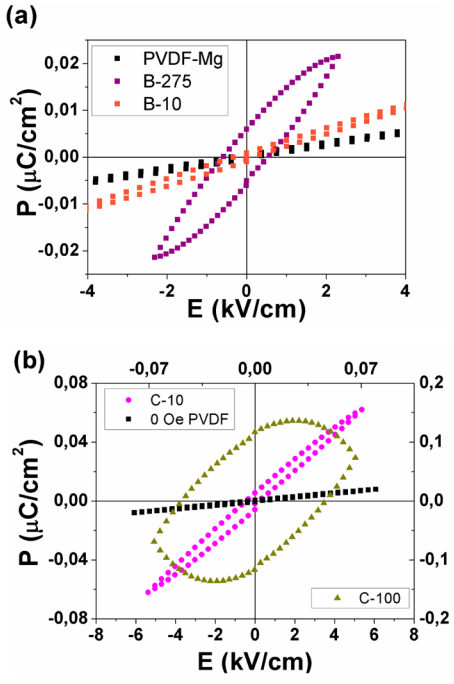

Figure 5. Dielectric polarization curves. **P**: dielectric moment per unit volume. **E**: electric field. (a) B−W W = 0, 10, 275. (b) C−W for W = 0, 10, 100.

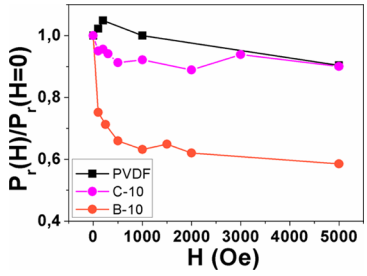

Figure 6. $P_R(\mathbf{H})/P_R(H = 0)$ vs **H**, where $P_R \equiv \mathbf{P}(E = 0)$. **H**: external magnetic field.

For instance, Lee et al.[35] conclude on the bases of neutron scattering experiments that the origin of the magnetoelectric coupling in $BiFeO_3$ are magnetostriction effects, since the presence of magnetic field decreases the distances between Bi, Fe, and O ions, producing a decreases of polarization at the unit cell, thus the magnetostriction. These effects may induce changes at ceramic-polymer interfaces which may generate subsequent perturbation of the ferroelectric order.

The following analysis is based on the assumption that magnetostriction is at the origin of magneto-electric coupling:

The **EM**-coupling coefficient, α, is defined by

$$\alpha \equiv \left(\frac{\partial \mathbf{P}}{\partial \mathbf{H}}\right)_{\mathbf{E}} \quad (1)$$

$\boldsymbol{\alpha}$, is experimentally determined by recording **P**−**E** curves in the presence of different magnetic fields **H**. Of course α is a function of **E** and **H**, but is currently determined at **E** = 0 actually, by calculating the dependence of the remanence polarization $P_R \equiv \mathbf{P}(E = 0, \mathbf{H})$ as a function of **H**. Martins et al.[36] indicated that determinations of α can be used to estimate the magnitude magnetostriction effects, that is strains (λ) induced by **H**, in the direction parallel to **H** (note that Martins et al. defined $\boldsymbol{\alpha}$ in a slightly different manner as $\left(\frac{\partial E_{induced}}{\partial H}\right)_E$ where $E_{induced}$ is the electric field induced by the polarization **P**, while **E** is the external field applied on the sample). Van den Boomgaard et al.[37] and Martins et al.[36] proposed that in composites where the matrix presents a ferroelectric character and the filler particles magnetostriction effects, then the **EM**-coupling is generated by geometrical distortions at a microscopic level induced by **H**, perturbing the electrical dipoles.

Within that frame, Van den Boomgaard et al. suggested the following model for $\boldsymbol{\alpha}$ is expressed by eq 2:

DOI: 10.1021/acs.jpcc.7b07800
J. Phys. Chem. C 2017, 121, 27683−27692

$$\alpha = \varphi_{matrix}\left(\frac{\partial \mathbf{P}}{\partial \lambda}\right)_{\mathbf{E}} \varphi_{filler}\left(\frac{\partial \lambda}{\partial \mathbf{H}}\right)_{\mathbf{E}} \quad (2)$$

where φ_{matrix} and φ_{filler} are the volume fractions of matrix and filler particles, respectively, $\varphi_{matrix} + \varphi_{filler} = 1$.

The term, $\varphi_{filler}\left(\frac{\partial \lambda}{\partial \mathbf{H}}\right)_{\mathbf{E}}$, accounts for magnetostriction induced by the filler. Here λ represents a strain at a microscopic level (λ has no units; positive λ indicates elongation in the direction of $\mathbf{H}$, while negative λ values indicates shrinkage). That is, the strain λ is induced by the action of the magnetic intensity, $\mathbf{H}$, hence $\lambda = 0$ when $\mathbf{H} = 0$. The proposal of Martins et al.[36] is that the magnetostriction coefficient, $\left(\frac{\partial \lambda}{\partial \mathbf{H}}\right)_{\mathbf{E}}$, can be estimated from eq 2.

The first term, $\varphi_{matrix}\left(\frac{\partial \mathbf{P}}{\partial \lambda}\right)_{\mathbf{E}}$, represents the piezoelectric contribution of the matrix, associated with the piezoelectric response of PVDF. The factor $\left(\frac{\partial \mathbf{P}}{\partial \lambda}\right)_{\mathbf{E}}$, the change of dielectric polarization when a strain appears, can be estimated from the following consideration. First, it is assumed that the induction of λ by $\mathbf{H}$ can be formally associated with a microscopic stress, T, parallel to $\mathbf{H}$. This is expressed by eq 3:

$$\left(\frac{\partial \mathbf{P}}{\partial \lambda}\right)_{\mathbf{E}} = \left(\frac{\partial \mathbf{P}}{\partial \mathbf{T}}\right)_{\mathbf{E}}\left(\frac{\partial \mathbf{T}}{\partial \lambda}\right)_{\mathbf{E}} \quad (3)$$

The next assumption is that λ and $\mathbf{T}$ are connected through the same relationship that at a macroscopic levels, that is, Young's modulus:

$$\mathbf{E}_Y \equiv \left(\frac{\partial \mathbf{T}}{\partial \lambda}\right)_{\mathbf{E}} \quad (4)$$

where, $\mathbf{E}_Y$, represents Young's modulus of the composite in the direction of $\mathbf{H}$ ($\mathbf{E}_Y \approx 2$ GPa for PVDF[38,39]). Additionally, $\mathbf{P}$ and T are related by the piezoelectric coefficient, d_{33}, according to

$$d_{33} \equiv \left(\frac{\partial \mathbf{P}}{\partial \mathbf{T}}\right)_{\mathbf{E}} \quad (5)$$

In a first approximation the parameters $\mathbf{E}_Y$ and d_{33} are assumed to be equal to the values determined by macroscopic determinations. For instance, in the case of $\mathbf{E}_Y$, it is assumed that $\mathbf{E}_Y$ in eq 3 can be estimated from determinations of stress–strain curves of the composite. This kind of hypothesis is usually referred as the *affine assumption*.[40] Additionally, $\mathbf{E}_Y$ and d_{33} are supposed to be constants, independent of λ. In the case of $\boldsymbol{E}_Y$, this assumption represents the definition of Young's modulus. Finally, we assume that $\boldsymbol{E}_Y$ and $\boldsymbol{d}_{33}$ are determined mainly by PVDF, with negligible influence of filler particles.

Therefore, the magnetostriction derivative is estimated according to

$$\left(\frac{\partial \lambda}{\partial \mathbf{H}}\right)_{\mathbf{E}} = \frac{\alpha}{\varphi_{filler}(1 - \varphi_{filler})d_{33}\mathbf{E}_Y} \quad (6)$$

there is just a formal difference when comparing to the expressions presented in Martins et al.[36] since those author expresses $\mathbf{P}$ in the CGS units, volts·.cm^{-1}, while here in MKSI, coulomb·m^{-2}).

Although, as mentioned above, α is dependent on $\mathbf{E}$ and $\mathbf{H}$, some approximations can be made. First, from the experimental point of view $\boldsymbol{\alpha}$ can be estimated *at remanence*, that is at $\mathbf{E} = 0$. Second, at relative low magnetic fields, $\boldsymbol{\alpha}$ can be assumed independent of $\mathbf{H}$. This was assumed by Martins et al. and seems to be already the situation experimentally observed in this work for $\mathbf{H}$ lower than a given value, above which there is saturation of the magnetostictive response (plateau). This implies that the slope of $P_R(\mathbf{H})/P_R(\mathbf{H} = 0)$ as a function of $\mathbf{H}$ is assume approximately constant at low $\mathbf{H}$ (see Figure 6). Therefore, if these hypotheses are incorporated, then the strain $\boldsymbol{\lambda}(\mathbf{H}, \mathbf{E} = 0)$ as a function of $\mathbf{H}$ can be calculated, at low $\mathbf{H}$, by integrating eq 6 with $\lambda(\mathbf{H} = 0, \mathbf{E} = 0) = 0$:

$$\boldsymbol{\lambda}(\mathbf{H}, \mathbf{E} = 0) = \frac{\alpha(\mathbf{E} = 0)\mathbf{H}}{\varphi_{filler}(1 - \varphi_{filler})d_{33}\mathbf{E}_Y} \text{ (for } \mathbf{H} \text{ below saturation)} \quad (7)$$

It is important to remark that PVDF has negative piezoelectric coefficient: $d_{33} < 0$ for PVDF ($d_{33} \approx -30$ pm V^{-1} [41]). Therefore, for PVDF an increase of λ renders to a decrease of $\mathbf{P}$; hence, the piezoelectric factor, $\left(\frac{\partial \mathbf{P}}{\partial \lambda}\right)_{\mathbf{E}}$ is negative for PVDF. Quantum calculations by Bystrov et al.[42] suggests that negative d_{33} on β-phase PVDF is related to redistribution of the electron molecular wave functions, leading to the shifting of atomic nuclei and reorganization of all total charges under an external strain.

Additionally, in the composites studied in the present work is $\boldsymbol{\alpha} < 0$ (negative EM coupling)), hence eqs 6 and 7 indicates positive magnetostriction effects for composites with $d_{33} < 0$. That is, the model predicts positive $\boldsymbol{\lambda}$ values which increase with $\mathbf{H}$ in $BiFeO_3$/PVDF and $CoFe_2O_4$/PVDF (positive magnetostriction).

A draft estimation of the induced strain and magnetostrictive effects, at low $\mathbf{H}$, $\lambda(\mathbf{H}, \mathbf{E} = 0)$, can be made from eq 7 by using the data of Figure 6 to evaluate $\alpha(\mathbf{E} = 0, \mathbf{H})$.

For instance, for samples B-10, the regime where $\boldsymbol{\alpha}$ is approximately constant correspond to $\mathbf{H} \leq 100$ Oe. From the experimental data it is $\boldsymbol{\alpha} \approx 2 \times 10^{-13}$ C cm^{-2} Oe^{-1} for $\mathbf{H} \leq 100$ Oe. With $\varphi_{filler} \approx 10^{-2}$, $\varphi_{matrix} \approx 1$, $d_{33} \approx -30$ pm V^{-1} and $\mathbf{E}_Y \approx 2$ GPa, then $\left(\frac{\partial \lambda}{\partial \mathbf{H}}\right)_{\mathbf{E}} \approx 3 \times 10^{-6}$ Oe^{-1}. Thus, $\lambda(\mathbf{H} = 100$ Oe, $\mathbf{E} = 0) \approx 300 \times 10^{-6}$ for B-10 is estimated.

For C-10, the range for linear variation of $\boldsymbol{\alpha}$ with $\mathbf{H}$ was found also for $\mathbf{H} \leq 100$ Oe with $\alpha \approx 5 \times 10^{-13}$ C cm^{-2} Oe^{-1} and $\lambda(\mathbf{H} = 100$ Oe, $\mathbf{E} = 0) \approx 700 \times 10^{-6}$. These crude estimations ($\lambda \sim 10^2$ ppm at low $\mathbf{H}$) are in the order of magnitude reported previously for related composites.[36]

It is also interesting to compare the **ME** coupling of $BiFeO_3$ in styrene–butadiene–rubber (SBR) and PVDF. In $BiFeO_3$/SBR composites, the coupling is always positive, $\mathbf{P}$ increases with $\mathbf{H}$, although it was only clearly observed in samples that were electrically or magnetically poled during preparation (and for $W \geq 50$).[8] In those poled $BiFeO_3$/SBR composites there is an almost linear increase of P_R with $\mathbf{H}$, while for $BiFeO_3$/PVDF and $CoFe_2O_4$/PVDF a decrease in P_R was observed which is not monotonous with $\mathbf{H}$ but it reaches a plateau. The different signs of the magnetoelectric coupling in SBR (positive) and PVDF (negative) when using $BiFeO_3$ as filler could be interpreted in the following way. Note that in $BiFeO_3$/SBR it is $\boldsymbol{\alpha} > 0$ and $d_{33} > 0$, while it is $\boldsymbol{\alpha} < 0$ and $d_{33} < 0$ in $BiFeO_3$/PVDF, predicting $\left(\frac{\partial \lambda}{\partial \mathbf{H}}\right)_{\mathbf{E}} > 0$ in both cases from eq 6. This is interesting since, as it has been mentioned above, there are many reports of negative magnetostriction are predicted by

DOI: 10.1021/acs.jpcc.7b07800
J. Phys. Chem. C 2017, 121, 27683–27692

quantum mechanical calculations of the crystalline structure for $CoFe_2O_4$ and $BiFeO_3$. However, the filler particles considered in the present work are aggregates (~200−500 nm size) formed by hundred of nanoparticles (~30 nm). This is in agreement with the possibility of large size effects in these composites, with a possible change of regime form negative magnetostriction for monocrystals to positive magnetostriction for aggregates. In fact, important effects on the **P**−**E** plots of functionalized $BiFeO_3$/PVDF have been recently reported by *Mishra et al.*[32] which may be associated with size and charge distributions of the dispersed filler.

4. CONCLUSIONS

The main effects of dispersing $BiFeO_3$ or $CoFe_2O_4$ particles in PVDF are (i) to increase the β-phase proportion, (ii) to induce dipoles and charge distributions, (iii) to increase the **P**−**E** response at low ceramic proportions (low-*W* group), (iv) to induce leakage currents above a concentration threshold (high-*W* groups), and (v) negative **EM** coupling at relatively low proportions of particles is observed.

The effects on the ferroelectric order when adding ferroic compounds like $BiFeO_3$ or $CoFe_2O_4$ is actually an open issue and still controversial in the literature, since several factors must be considered with possible opposite effects: perturbation of the different phases of the polymer, increasing interfaces, addition of dipoles and charges, etc (see for instance Martins et al.[20]). However, our results are very conclusive: addition of $BiFeO_3$ or $CoFe_2O_4$ increases the β-phase proportion and the dielectric polarization. Dielectric polarization increases up to filler concentration values where leakage currents induce large distortions of polarizations curves, avoiding further analysis of **P**−**E** plots and **ME** effects in the large-W group. This description is in full agreement with the presented results of impedance spectroscopy analysis.

The **ME** constant, $\boldsymbol{\alpha}$, has opposite signs in $BiFeO_3$/PVDF and $BiFeO_3$/SBR composites. This is consistent with positive magnetostriction effects, $\left(\frac{\partial\lambda}{\partial \mathbf{H}}\right)_{\mathbf{E}} > 0$, in both cases.

The negative magneto-electric coupling indicates that the system can change from a more ferroelectric-like behavior toward a more paraelectric-like material. This suggests that application of magnetic fields in systems with large negative magneto-electric coupling could substantially reduce the electric hysteresis, erasing the electric memory. That is, the magnetic field could convert the composite from a ferroelectric capacitor to a dielectric one. Concerning possible applications, first it is important to note that the values of **P** reported here are in the same order of magnitude than those reported by other authors, in the range 10^{-2}−10^{-1} μC cm^{-2}, depending of filler concentration. But for many practical applications is necessary to increase **P** by increasing filler concentration without increasing leakage currents. In other words, the challenge for going beyond in applications is to design systems with improved filler dispersion, increasing its proportion in the composite while avoiding percolation. For instance, adding surfactants with different surface charges may favor dispersion in the matrix. Actually we have added SDS when preparing the $BiFeO_3$/PVDF composites, but without observing improve in the dielectric response. Recently Misha et al.[36] reported on a very promising approach based on including a previous step by hydroxylating the surfaces of $BiFeO_3$ adding hydrogen peroxide as modifying agent which induce polar functional groups, and adding the surfactant only after hydroxylation. This kind of approach must be considered in future works in these composites.

■ ASSOCIATED CONTENT

Supporting Information

The Supporting Information is available free of charge on the ACS Publications website at DOI: 10.1021/acs.jpcc.7b07800.

FTIR spectra, illustrating the effect of increase the β-phase of PVDF after adding a salt and filler particles, fits of several dielectric functions as a function of frequency (extracted form impedance analysis spectroscopy) for different filler/PVDF composites, and real and imaginary parts of dielectric constants (PDF)

■ AUTHOR INFORMATION

Corresponding Author

*(R.M.N.) E-mail: rmn@qi.fcen.uba.ar. Telephone: +54-11-4576-3358. Fax: xx54-11-4576-3341.

ORCID

R. Martín Negri: 0000-0003-4404-0592

Notes

The authors declare no competing financial interest.

■ ACKNOWLEDGMENTS

R.M.N. is a professor at the University of Buenos Aires (UBA) and research member of the National Council of Research and Technology (CONICET, Argentina). L.M.S.M. is a postdoctoral fellow of CONICET. Financial support was received from UBA (UBACyT Project 20020150100079BA 2017/2019) and Ministry of Science, Technology and Innovations (MINCYT-FONCYT, Argentina, PICT 2011-0377). The Center of Advanced Microscopy (CMA), UBA, is acknowledged for the SEM-AFM images. The Laboratory of Low-Temperatures, Department of Physics, School of Sciences, UBA, is acknowledged for magnetic measurements.

■ REFERENCES

(1) Wong, W. S.; Salleo, A. *Flexible electronics: materials and applications*; Electronic Materials: Science & Technology 11; Springer Science & Business Media: 2009.

(2) Mietta, J. L.; Ruiz, M. M.; Antonel, P. S.; Perez, O. E.; Butera, A.; Jorge, G.; Negri, R. M. Anisotropic magnetoresistance and piezoresistivity in structured Fe_3O_4-silver particles in PDMS elastomers at room temperature. *Langmuir* **2012**, *28*, 6985−6996.

(3) Ausanio, G.; Iannotti, V.; Ricciardi, E.; Lanotte, L.; Lanotte, L. Magneto-piezoresistance in Magnetorheological elastomers for magnetic induction gradient or position sensors. *Sens. Actuators, A* **2014**, *205*, 235−239.

(4) Yang, K.; Huang, X.; Huang, Y.; Xie, L.; Jiang, P. Fluoropolymer@ $BaTiO_3$ hybrid nanoparticles prepared via RAFT polymerization: toward ferroelectric polymer nanocomposites with high dielectric constant and low dielectric loss for energy storage application. *Chem. Mater.* **2013**, *25*, 2327−2338.

(5) Mietta, J. L.; Jorge, G.; Perez, O. E.; Maeder, T.; Negri, R. M. Superparamagnetic anisotropic elastomer connectors exhibiting reversible magneto-piezoresistivity. *Sens. Actuators, A* **2013**, *192*, 34−41.

(6) Ruiz, M. M.; Marchi, M. C.; Perez, O. E.; Jorge, G.; Fascio, M.; D'Accorso, N.; Negri, R. M. Structured elastomeric submillimeter films displaying magneto and piezo resistivity. *J. Polym. Sci., Part B: Polym. Phys.* **2015**, *53*, 574−586.

(7) Antonel, S. P.; Jorge, G.; Perez, O. E.; Butera, A.; Leyva, G. A.; Negri, R. M. Magnetic and elastic properties of $CoFe_2O_4$-

DOI: 10.1021/acs.jpcc.7b07800
J. Phys. Chem. C 2017, 121, 27683−27692

polydimethylsiloxane magnetically oriented elastomer nanocomposites. *J. Appl. Phys.* **2011**, *110*, 043920.
(8) Saleh Medina, L. M.; Jorge, G.; Rubi, D.; D'Accorso, N.; Negri, R. M. SBR/$BiFeO_3$ elastomer capacitor films prepared under magnetic and electric fields displaying magnetoelectric coupling. *J. Phys. Chem. C* **2015**, *119*, 23319−23328.
(9) Gregorio, R. Determination of the α, β, and γ crystalline phases of poly(vinylidene fluoride) films prepared at different conditions. *J. Appl. Polym. Sci.* **2006**, *100*, 3272−3279.
(10) He, X.; Yao, K. Crystallization mechanism and piezoelectric properties of solution-derived ferroelectric poly(vinylidene fluoride) thin films. *Appl. Phys. Lett.* **2006**, *89*, 112909.
(11) Chen, S.; Yao, K.; Tay, F. E. H.; Liow, C. L. Ferroelectric poly (vinylidene fluoride) thin films on Si substrate with the beta phase promoted by hydrated magnesium nitrate. *J. Appl. Phys.* **2007**, *102*, 104108.
(12) Sun, L.; Li, B.; Zhang, Z.; Zhong, W. H. Achieving very high fraction of β-crystal PVDF and PVDF/CNF composites and their effect on a-c conductivity and microstructure through a stretching process. *Eur. Polym. J.* **2010**, *46*, 2112−2119.
(13) Yu, L.; Cebe, P. Effect of nanoclay on relaxation of poly (vinylidene fluoride) nanocomposites. *J. Polym. Sci., Part B: Polym. Phys.* **2009**, *47*, 2520−2532.
(14) Luo, B.; Wang, X.; Wang, Y.; Li, L. Fabrication, characterization, properties and theoretical analysis of ceramic/PVDF composite flexible films with high dielectric constant and low dielectric loss. *J. Mater. Chem. A* **2014**, *2*, 510−519.
(15) Thomas, P.; Varughese, K.; Dwarakanath, K.; Varma, K. Dielectric properties of poly (vinylidene fluoride)/$CaCu_3Ti_4O_{12}$ composites. *Compos. Sci. Technol.* **2010**, *70*, 539−545.
(16) Dang, Z. M.; Shen, Y.; Nan, C. W. Dielectric behavior of three-phase percolative Ni−$BaTiO_3$/polyvinylidene fluoride composites. *Appl. Phys. Lett.* **2002**, *81*, 4814−4816.
(17) Reddy, A. V.; Sekhar, K.; Dabra, N.; Nautiyal, A.; Hundal, J. S.; Pathak, N.; Nath, R. Ferroelectric and magnetic Properties of hot-pressed $BiFeO_3$-PVDF composite films. *ISRN Mater. Sci.* **2011**, *2011*, 1.
(18) Moharana, S.; Mishra, M.; Behera, B.; Mahaling, R. A. Comparative study of dielectric properties of calcined and un-calcined $BiFeO_3$-poly(vinylidene fluoride)(PVDF) composite films. *Int. J. Eng. Technol. Manag. Appl. Sci.* **2015**, *3*, 303.
(19) Martins, P.; Costa, C. M.; Lanceros-Mendez, S. Nucleation of electroactive β-phase poly(vinilidene fluoride) with $CoFe_2O_4$ and $NiFe_2O_4$ nanofillers: a new method for the preparation of multiferroic nanocomposites. *Appl. Phys. A: Mater. Sci. Process.* **2011**, *103*, 233−237.
(20) Martins, P.; Moya, X.; Phillips, L. C.; Kar-Narayan, S.; Mathur, N. D.; Lanceros-Mendez, S. Linear anhysteretic direct magnetoelectric effect in $Ni_{0.5}Zn_{0.5}Fe_2O_4$ /poly(vinylidene fluoride-trifluoroethylene) 0−3 nanocomposites. *J. Phys. D: Appl. Phys.* **2011**, *44*, 482001−482005.
(21) Martins, P.; Moya, X.; Caparrós, C.; Fernandez, J.; Mathur, N.; Lanceros-Mendez, S. Large linear anhysteretic magnetoelectric voltage coefficients in $CoFe_2O_4$/polyvinylidene fluoride 0−3 nanocomposites. *J. Nanopart. Res.* **2013**, *15*, 1−6.
(22) Saleh Medina, L. M.; Jorge, G.; Negri, R. M. Structural, dielectric and magnetic properties of $Bi_{(1-x)}Y_xFeO_3$ ($0 < x < 0.2$) obtained by acid−base co-precipitation. *J. Alloys Compd.* **2014**, *592*, 306−312.
(23) Ruiz, M. M.; Mietta, J. L.; Antonel, P. S.; Pérez, O. E.; Negri, R. M.; Jorge, G. Structural and magnetic properties of $Fe_{2-x}CoSm_xO_4$—nanoparticles and $Fe_{2-x}CoSm_xO_4$—PDMS magnetoelastomers as a function of Sm content. *J. Magn. Magn. Mater.* **2013**, *327*, 11−19.
(24) Barsoukov, E.; Macdonald, J. R. *Impedance spectroscopy: theory, experiment, and applications*. John Wiley & Sons: 2005.
(25) Yu, S.; Zheng, W.; Yu, W.; Zhang, Y.; Jiang, Q.; Zhao, Z. Formation mechanism of β-phase in PVDF/CNT composite prepared by the sonication method. *Macromolecules* **2009**, *42*, 8870−8874.
(26) Martins, P.; Caparros, C.; Gonçalves, R.; Martins, P. M.; Benelmekki, M.; Botelho, G.; Lanceros-Mendez, S. Role of nanoparticle surface charge on the nucleation of the electroactive β-poly(vinylidene fluoride) nanocomposites for sensor and actuator applications. *J. Phys. Chem. C* **2012**, *116*, 15790−15794.
(27) Tsangaris, G.; Psarras, G.; Kouloumbi, N. Electric modulus and interfacial polarization in composite polymeric systems. *J. Mater. Sci.* **1998**, *33*, 2027−2037.
(28) Dash, S.; Choudhary, R. N. P.; Goswami, M. N. Enhanced dielectric and ferroelectric properties of PVDF-$BiFeO_3$ composites in 0−3 connectivity. *J. Alloys Compd.* **2017**, *715*, 29−36.
(29) Dickens, B.; Balizer, E.; DeReggi, A.; Roth, S. Hysteresis measurements of remanent polarization and coercive field in polymers. *J. Appl. Phys.* **1992**, *72*, 4258−4264.
(30) Ducharme, S.; Fridkin, V. M.; Bune, A. V.; Palto, S. P.; Blinov, L. M.; Petukhova, M. N.; Yudin, S. G. Intrinsic ferroelectric coercive field. *Phys. Rev. Lett.* **2000**, *84*, 175.
(31) Gan, W. C.; Abd. Majid, W. H. Enhancing pyroelectric and ferroelectric properties of PVDF composite thin films by dispersing a non-ferroelectric inclusion La_2O_3 for application in sensors. *Org. Electron.* **2015**, *26*, 121−128.
(32) Mishra, M. K.; Moharana, S.; Mahaling, R. N. Enhanced dielectric properties of poly(vinylidene fluoride)−surface functionalized $BiFeO_3$ composites using sodium dodecyl sulfate as a modulating agent for device applications. *J. Appl. Polym. Sci.* **2017**, *134*, 45040.
(33) Anithakumari, P.; Mandal, B. P.; Abdelhamid, E.; Naik, R.; Tyagi, A. K. Enhancement of dielectric, ferroelectric and magneto-dielectric properties in PVDF−BaFeO composites: a step towards miniaturizated electronic devices. *RSC Adv.* **2016**, *6*, 16073−16080.
(34) Nan, C. W. Magnetoelectric effect in composites of piezoelectric and piezomagnetic phases. *Phys. Rev. B: Condens. Matter Mater. Phys.* **1994**, *50*, 6082.
(35) Lee, S.; Fernandez-Diaz, M. T.; Kimura, H.; Noda, Y.; Adroja, D. T.; Lee, S.; Park, J.; Kiryukhin, V.; Cheong, S. W.; Mostovoy, M.; Park, J.-G. Negative magnetostrictive magnetoelectric coupling of $BiFeO_3$. *Phys. Rev. B: Condens. Matter Mater. Phys.* **2013**, *88*, 060103.
(36) Martins, P.; Silva, M.; Lanceros-Mendez, S. Determination of the magnetostrictive response of nanoparticles via magnetoelectric measurements. *Nanoscale* **2015**, *7*, 9457−9461.
(37) Van Den Boomgaard, J.; Van Run, A. M. J. G.; Van Suchtelen, J. Magnetoelectricity in piezoelectric-magnetostrictive composites. *Ferroelectrics* **1976**, *10*, 295−298.
(38) Broadhurst, M. G.; Davis, G. T. Physical basis for piezoelectricity in PVDF. *Ferroelectrics* **1984**, *60*, 3−13.
(39) Greco, F.; Zucca, A.; Taccola, S.; Menciassi, A.; Fujie, T.; Haniuda, H.; Takeoka, S.; Dario, P.; Mattoli, V. Ultra-thin conductive free-standing PEDOT/PSS nanofilms. *Soft Matter* **2011**, *7*, 10642−10650.
(40) Mietta, J. L.; Tamborenea, P. I.; Negri, R. M. Anisotropic reversible piezoresistivity in magnetic-metallic/polymer structured elastomer composites: modelling and experiments. *Soft Matter* **2016**, *12*, 422−431.
(41) Kepler, R. G. Ferroelectric polymers. In *Ferroelectric Polymers: Chemistry: Physics, and Applications*; Nalwa, H. S., Eds.; Marcel Dekker: New York, 1995; Chapter 3.
(42) Bystrov, V. S.; Paramonova, E. V.; Bdikin, I. K.; Bystrova, A. V.; Pullar, R. C.; Kholkin, A. L. Molecular modeling of the piezoelectric effect in the ferroelectric polymer poly(vinylidene fluoride) (PVDF). *J. Mol. Model.* **2013**, *19*, 3591−3602.

DOI: 10.1021/acs.jpcc.7b07800
J. Phys. Chem. C 2017, 121, 27683−27692